
Review

Electrospun polytetrafluoroethylene (PTFE) fibers in membrane distillation applications

Charles Defor¹ and Shih-Feng Chou^{2,*}

¹ Department of Chemical Engineering, College of Engineering, The University of Texas at Tyler, 3900 University Blvd., Tyler, TX 75799, USA

² Department of Mechanical Engineering, College of Engineering, The University of Texas at Tyler, 3900 University Blvd., Tyler, TX 75799, USA

* **Correspondence:** Email: schou@uttyler.edu; Tel: +1-903-566-6209.

Abstract: Polytetrafluoroethylene (PTFE) is a fully fluorinated linear polymer with a $(CF_2-CF_2)_n$ backbone. High molecular weight PTFEs are chemically inert while possessing excellent hydrophobic surface properties attributed to their low surface energy. These characteristics make PTFE an excellent candidate for membrane distillation application among all other hydrophobic polymers. In this review, the electrospinning processes of PTFE fibers are discussed in detail with a focus on various electrospinning effects on the resulting fiber morphologies and structures. Due to the high chemical resistance and low solvent solubility, PTFE is typically electrospun with a polymer carrier, such as polyvinyl alcohol (PVA) and/or polyethylene oxide (PEO), using emulsion electrospinning followed by a sintering process. The amount of PTFE in emulsion, types of polymer carriers, electrospinning parameters, and sintering conditions have interconnected effects on the resulting morphological structures of PTFE fibers (e.g., beading or continuous fibers). In addition, electrospun PTFE fibers are further functionalized using methods of co-electrospinning with other hydrophobic polymers as well as incorporations of metallic (ZnO) and inorganic particles (POSS) to improve their performance in membrane distillation. Water contact angles, permeation fluxes, salt rejection rates, and hours of operations are reported for various functionalized electrospun PTFE fibrous membranes to demonstrate their feasibility in membrane distillation applications. In general, this article provides a scientific understanding of electrospun PTFE fibers and their engineering application in membrane distillation.

Keywords: PTFE; Teflon; fibers; emulsion electrospinning; membrane distillation; water contact angles; permeation fluxes; salt rejection rates

1. Introduction

Polytetrafluoroethylene (PTFE), commercially known as Teflon, is a fully fluorinated polymer derived from the monomer of tetrafluoroethylene (TFE) with the molecular formula $(CF_2-CF_2)_n$ [1]. It is known for its white appearance, hydrophobic surface properties, and chemical resistance. It showcases properties heavily reliant on its molecular weight. For example, high molecular weight PTFE remains chemically inert and insoluble in various solvents, including hot fluorinated liquids. PTFE is synthesized through conventional-radical polymerization and typically adopts a linear chain structure without branches or loop formations [2]. The helical conformation of PTFE is influenced by polymerization conditions, such as temperature and pressure [3]. This helical structure imparts a rigid and rodlike character to the polymer chain, leading to crystallites characterized by large regions of long, straight, and ordered chain packing. Such arrangement contributes to the high crystallinity observed in both virgin and sintered PTFE. Different initiation methods may yield variations in microstructure, such as branching seen in PTFE synthesized via γ radiation initiation [4]. It exhibits a semi-crystalline nature owing to its high molecular weight and is resistant to chemicals due to the strong C–F bond [5,6]. Figure 1 shows the radical polymerization process of PTFE forming a linear and helical conformation with a carbon backbone surrounded by fluorine atoms.

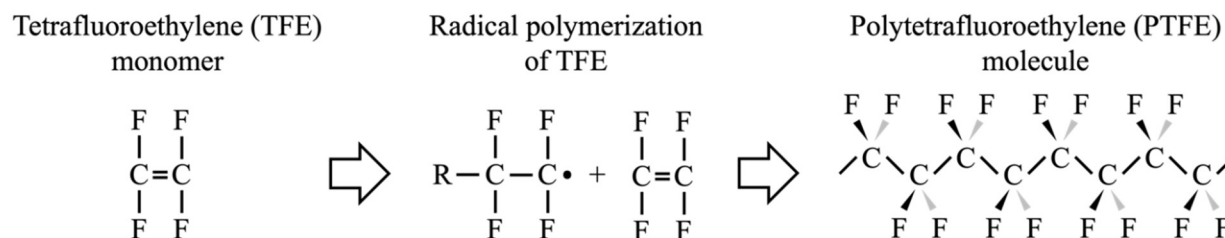


Figure 1. Schematic of the PTFE molecular structure and its polymerization process from TFE monomers.

Membrane distillation (MD) presents a promising avenue for desalination powered by thermal energy. This process requires a hydrophobic membrane that selectively allows pure water to permeate through the membrane in the form of vapor while repelling the remaining impurities [7]. In MD, saline feedwater is heated and passed over a microporous hydrophobic membrane, prompting vaporization and subsequent passages through the membrane's pores, driven by the vapor pressure differences between the feed and permeate sides. This yields a vapor-liquid interface across the membrane pores, allowing volatile substances to evaporate, diffuse, and/or convect across the membrane before condensing or being eliminated on the opposite side. There are four main MD configurations, as shown in Figure 2 [8]: (a) direct contact membrane distillation (DCMD), where the permeating side is a condensing fluid in direct contact with the membrane; (b) air gap membrane distillation (AGMD), where an air gap separates the condensing surface from the membrane allowing vaporized solvents to be recovered; (c) sweep gas membrane distillation (SGMD), where vaporized solvent is removed by a

sweep gas; and (d) vacuum membrane distillation (VMD), where the vaporized solvent is recovered under vacuum.

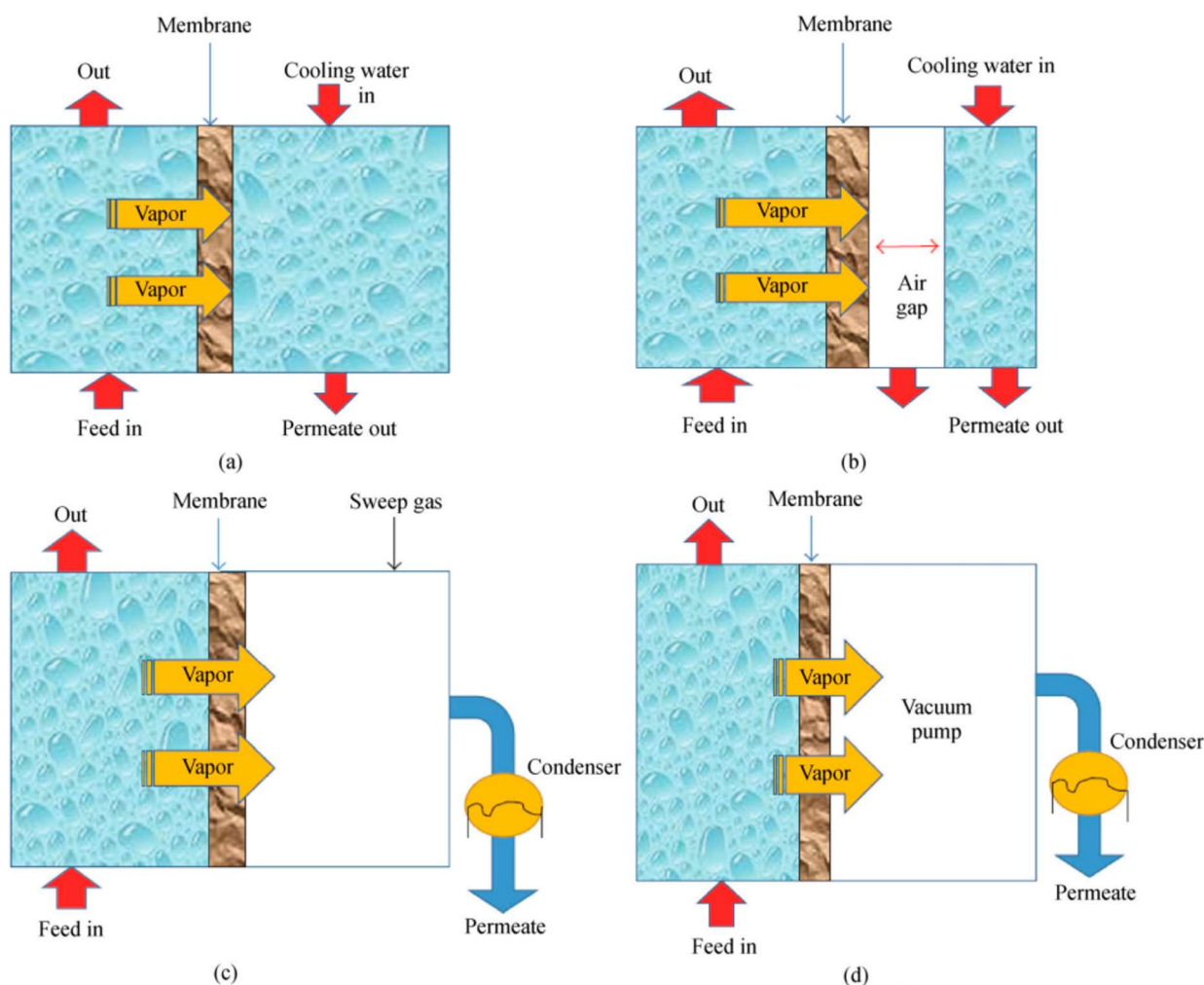


Figure 2. Schematic of four main MD configurations, including (a) DCMD, (b) AGMD, (c) SGMD, and (d) VMD (Reproduced from Ref. [8] with permission).

In DCMD, a hot feed solution is brought into contact with the membrane, and evaporation produces a gas phase driven by pressure difference to the permeate side of the membrane. Due to the hydrophobic nature of the membrane, only the gas phase can move across to the permeate side of the membrane. In VMD, a pump creates a vacuum that causes vapor molecules to be sucked out at the permeate side, and condensation occurs outside the membrane module. In AGMD, feed solutions are brought into contact with the hot side of the membrane, and stagnant air is introduced between the membrane and condensation surface; vapor moves across the air gap to condense over the cold surface inside the membrane cell. In SGMD, inert gas is used to move vapor at the permeate membrane side to condense outside the membrane module. The main advantage of DCMD and VMD over AGMD and SGMD is that both have high permeate flux and are commercially viable; however, DCMD has a problem of conductive heat loss, which AGMD and SGMD solve. VMD has a problem with membrane pore wetting.

Various studies have demonstrated the performance of DCMD and VMD mentioned above. For example, Li et al. electrospun colloid solutions of polyvinylidene fluoride (PVDF) containing silica nanoparticles into fibrous membranes to study their DCMD performance over 24 h, and the results demonstrated a permeate flux of 41.1 kg/m²/h [9]. In comparison, Dong et al. electrospun superhydrophobic fibrous membranes using blend PVDF and PTFE solutions for VMD performance over 15 h, and the results showed a significantly lower permeate flux of 18.5 kg/m²/h [10]. While DCMD appeared to have a higher permeate flux than VMD when using the electrospun PVDF fibrous membranes, a direct comparison based on the permeate flux between these two methods may be insufficient. Silica nanoparticles have been shown to improve distillation performance by making the fiber surfaces more hydrophobic, surpassing the effect of blending with superhydrophobic polymers [11]. To better determine the performance of DCMD and VMD, Efome et al. reported permeate fluxes of 6.5 and 3.2 kg/m²/h from DCMD and VMD tests, respectively, using flat sheets of electrospun PVDF and silica nanoparticles composite membranes [12]. These composite fibrous membranes were more stable in the long-term testing of DCMD and VMD than those of the pristine silica nanoparticle-embedded PVDF fibers.

The selection of a suitable hydrophobic and microporous membrane is pivotal for effective MD. An optimal membrane should exhibit high permeability, low thermal conductivity, and high liquid entry pressure, alongside robust thermal stability and chemical resistance to feed streams. The process efficiency relies on optimizing mass and heat transfer, which are determined by the membrane's morphological and structural properties [13]. Organic membranes, widely used in industrial contexts, offer appealing characteristics including compactness, lightweight, and high packing density [14,15]. Among the commonly employed hydrophobic membrane materials, polypropylene (PP), PVDF, and PTFE membranes appear to be the ideal candidates for MD applications. These synthetic polymers boast exceptional chemical stability, heat resistance, hydrophobicity, and fracture toughness due to their high crystallization, strong C–C and C–F bonds, and a protective helical sheath formed by the electron clouds of outer fluorine atoms [16,17]. PTFE membranes are favored in MD due to their low thermal conductivity, hydrophobic nature, low liquid entry pressure, and suitable pore structure (~0.5 μm), which collectively minimize heat loss and facilitate efficient vapor transport [13].

With these advantages in MD, fabrications of the PTFE membranes are of particular interest, especially for fibrous membranes with average fiber diameters in the range of nano- to micro-scaled fibers. Specifically, electrospinning is ideal for producing small-diameter fibers with large surface area and pore size. The objective of this review is to provide an overview of the recent advancements and applications of electrospun PTFE membranes in MD. We briefly discuss the electrospinning principle and the processing parameters that affect the electrospun fibers. Moreover, PTFE fibers are produced by emulsion electrospinning, where a polymer carrier is typically used in the process followed by a sintering stage to remove it. More importantly, we review current works of electrospun PTFE fibers in MD on their properties and performance, including water contact angles, permeation fluxes, salt rejection rates, and hours of operation. In general, this article provides a review of the electrospinning of PTFE fibers while also illustrating the use of PEFT fibers in MD.

2. Membrane fabrication

During fabrication, two characteristics of membranes need to be considered: hydrophobicity and porosity. PTFE exhibits exceptionally good characteristics on both fronts. These membranes can be in

the form of unsupported, supported, composite dual-layer membranes, single-layer membranes, and composite triple-layer membranes. The mean pore size of membranes used in membrane distillation is between 10 nm and 1 μm . There are numerous methods for membrane fabrication, including track etching, phase inversion, sintering, and fiber electrospinning. Among these methods, phase inversion is the most prevalent method [18]. However, other membrane fabrication methods involve more than one method. For example, Xu et al. fabricated a membrane by combining extrusion, sintering, and stretching [19]. In phase inversion, a polymeric solution is solidified by processes such as evaporation-induced phase separation, thermally induced phase separation, non-solvent-induced phase separation, or vapor-induced phase separation in a controlled manner [20]. Among these, the non-solvent-induced phase separation and thermally induced phase separation methods are the most used. In the former, a polymer solution is cast on glass or support followed by putting them in a non-solvent bath. The solvent miscibility occurs until the whole polymeric solution becomes solid. In the thermally induced phase separation method, a diluent is used to make the polymer solution followed by a cooling process to precipitate the polymer. The removal of the diluent from the polymer solution results in pore formation [21,22].

However, in recent years, electrospun fiber membranes have emerged as a viable alternative to phase inversion methods in membrane distillation [23,24]. To make an electrospun nanofibrous membrane, a polymeric solution is poured into a syringe attached to a needle followed by setting them on a syringe pump to slowly dispense the polymer solution. A direct current voltage is applied to the needle and the collector to create the electric field to draw the polymer solution. When the applied electric field overcomes the surface tension of the polymer solution, a polymeric jet is formed and collected on a stationary collector or a rotating drum in the form of fiber mats. The electrospinning of various fibers has been documented in our previous works [25–30].

3. Electrospun fibers

The concept of producing artificial small-diameter fibers from electric charges has existed for many years. However, dried polymers/fibers at the tip of the collector due to fast solvent evaporation have made these attempts difficult [31]. Formhals first used an electric field to spin cellulose acetate in acetone [32]. The fiber spinning technique consisted of a mobile collecting device to collect fibers on rotating devices so that the unwinding of the fibers occurred continuously. However, the short distance between the spinneret and collector made it difficult for the fibers to dry. This process was further refined by altering the distance between the spinneret and collector. In 1969, Taylor introduced the fundamental concept of electrospinning by studying the jet formation process: the polymer droplet at the needle tip. A cone is formed when an electric field is applied between the needle tip and the collector, called the *Taylor cone*. Despite this, not much attention was given to this process until the 1990s [33], when the advent of new polymers and new applications of nanotechnology led researchers and universities to focus on electrospinning.

3.1. Electrospinning process description

The electrospinning process consists of three components, as shown in Figure 3: a high-voltage source, a needle with a syringe pump setup, and a metal collector [34]. The drawing of a polymer solution is driven by the applied electrical force over a distance. When a sufficiently high voltage is

attained, the electrical force overcomes the surface tension of the polymer solution at the tip of the needle, resulting in the deformation of the polymer droplet into a Taylor cone [33], leading to the ejection of the polymer solution in a thin jet. At first, the jet undergoes a short distance of stable stretching before undergoing an undefined bending and whipping (i.e., jet instability) that leads to polymer jet stretching with the effects of solvent evaporation and charge repulsion. The solidified fibers on the collector can attain diameters in the range of sub-microns, with various fiber orientations depending on the collectors used [35].

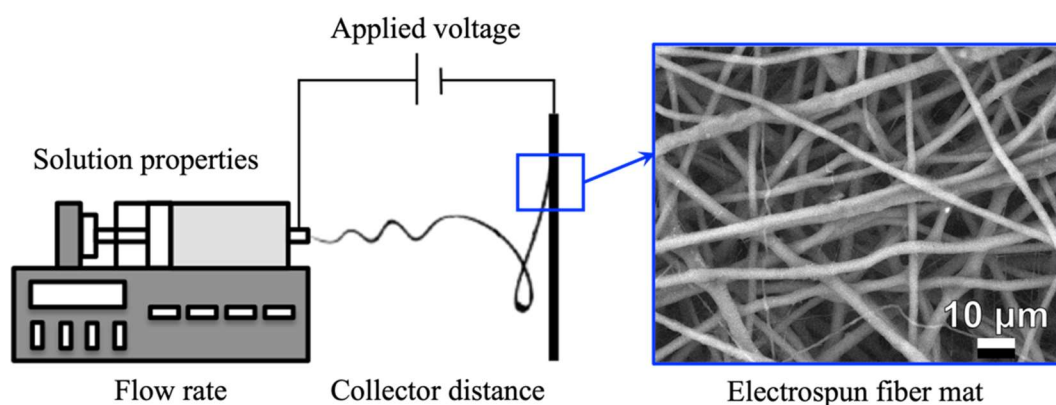


Figure 3. Schematic of the single nozzle electrospinning process using a stationary collector and the resulting fiber structure. The SEM image of the electrospun fibers was produced by the authors using polyester for representation purposes.

3.2. Operation parameters of electrospinning

The electrospinning technique is generally noted for its high output and low cost of nano/micro-sized fibers. In addition, the control of pore size in the fiber mats and fiber arrangements can be achieved with electrospinning. The electrospinning parameters can be divided into three major groups, namely (1) electrospinning parameters, (2) polymer solution parameters, and (3) environmental parameters. The following sections will briefly discuss these parameters.

3.2.1. Electrospinning parameters

Several groups have studied the effects of the applied voltages on electrospun fibers. For example, Beachley and Wen reported that polycaprolactone fiber length and fiber diameter decreased directly proportionally to the applied voltage [36]. However, the fiber diameter was the only outcome that decreased significantly with the applied voltage. In addition, an increase in applied voltage led to more uniform fibers. In another study, Yördem et al. studied the effects of applied voltages on the average fiber diameters of electrospun polyacrylonitrile fibers at various solution concentrations and collector distances [37]. Zhang et al. showed the effects of the applied voltage on the fiber diameter of polyvinyl alcohol (PVA) mats and found that there was an increase in fiber diameter with the increase of the applied voltage [38]. It can be summarized that the applied voltage influences fiber diameter, where a higher applied voltage leads to a smaller fiber diameter.

Another important electrospinning parameter is the flow rate of the polymer solution. A proper flow rate in combination with the appropriate applied voltage allows the generation of the polymer jet from the Taylor cone. For example, Zargam et al. studied the effects of flow rate on the morphology of nylon 6 [39]. Results showed that a small droplet formed at low flow rates, whereas a great amount of the polymers were electrospayed at higher flow rates.

In electrospinning, the tip-to-collector distance affects fiber morphology. If the distance is short, wet fibers have insufficient time to dry and solidify before reaching the collector. If the distance is too long, the number of beads can increase by a significant amount. Homayoni et al. reported that tip-to-collector distance had a direct influence on jet flight time and electric field strength [40]. A decrease in the collector distance reduces the flight time of the polymer jets, which minimizes the time for solvent evaporation before reaching the collector.

3.2.2. Polymer solution parameters

Preparation of the polymer solution is the first and most important step in making electrospun fibrous membranes. Polymers must be dissolved in the appropriate solvent; factors such as polymer concentrations and their molecular weights can significantly affect electrospinning and the resulting fiber morphology. These polymer solution properties include concentration, viscosity, conductivity, and surface tension.

Polymer concentration is a key parameter in electrospinning. Using a low polymer concentration typically leads to electrospaying rather than electrospinning. Tan et al. showed that the electrospun fiber diameter had a direct correlation with polymer concentrations [41]. The study also reported the minimum polymer concentration at which fiber electrospinning occurred. In another study, Liu et al. observed that polymer concentration affected the number of beads and the efficacy of the electrospinning process [42]. Finally, He et al. demonstrated that the fiber diameter of electrospun polyacrylonitrile fibers linearly depended on the corresponding polymer solution concentrations [43].

The viscosity of a polymer solution can be seen from its degree of polymer chain entanglement. The chain entanglement is a function of the molecular weight of the linear polymer. Koski et al. observed that fiber diameter increased with increasing polymer molecular weight [44]. Mit-uppatham et al. studied the effects of solution properties on the morphology and fiber diameters of as-spun polyamide-6 fibers [45]. Results showed that an increase in polymer concentration increased the solution viscosity, with polymer solutions transiting from low to high viscosity. Due to the increase of polymer solution viscosity, the electrospinning results changed from small droplets to a combination of droplets followed by fibers when reaching the critical viscosity in the polymer solution.

Surface tension of the polymer solution affects electrospinning and is directly influenced by the polymer solvent composition. Jarusuwannapoom et al. investigated the effect of 18 solvents on the morphological appearance of as-spun polystyrene fibers [46]. Results showed that lower values of surface tension were a good starting point for fiber electrospinning. Jia and Qin studied the effects of different surfactants on electrospinning of PVA [47]. Results demonstrated that surface tension decreased markedly when surfactant content was less than 1%. The fiber diameter of PVA fiber mats decreased from 405 to 100 nm in this range. This suggests that lower surface tension is desired in electrospinning.

The conductivity of a polymer solution affects charge density. When a polymer solution of low charge density is put into an electrospinning system, the applied voltage needs to be higher than usual

to generate the required surface tension for fiber formation [48]. Solution conductivity can be improved by adding ionic salts and/or organic acids to dope solutions, such as lithium chloride and sodium nitrate. Improving solution conductivity generally results in fibers with a more uniform diameter and smooth structure [49,50].

Solvent volatility has a considerable effect on fiber production and morphology. Low-volatility solvents typically form wet fibers. This defect can be offset by using highly volatile solvents. However, highly volatile solvents can lead to inconsistent electrospinning due to polymer solidification at the tip of the spinneret [51,52]. In addition, highly volatile solvents can form flat or ribbon-like fibers or even fibers with pore-on-surface structures [53,54].

3.2.3. Environmental parameters

Ambient conditions affect electrospinning, especially temperature and relative humidity. De Vrieze et al. investigated the effect of temperature and humidity on the properties and formation of electrospun cellulose acetate and polyvinylpyrrolidone fibers [55]. Results showed that the average fiber diameter was a function of relative humidity, which also influenced fiber morphology. Hardick et al. observed that levels of relative humidity were the most significant factor in beading during the electrospinning of cellulose acetate fibers [56]. The average fiber diameter of electrospun cellulose acetate fibers increased with increasing temperature and relative humidity.

4. Emulsion electrospinning of PTFE fibrous membranes

Direct electrospinning of PTFE fibers is difficult due to PTFE's thermal stability and high chemical resistance, rendering it almost impossible to obtain a PTFE solution for electrospinning. Also, high molecular weights are required to achieve sufficient mechanical strength since PTFE is a linear polymer without any branches and/or side groups for enhanced chain entanglements [57,58]. Such a high molecular weight gives rise to a high solution viscosity, which makes electrospinning of PTFE difficult [59].

To overcome the problem of low solubility of PTFE in various organic solvents and to avoid using highly toxic solvents to improve the solubility of PTFE, an environmentally friendly method, known as emulsion electrospinning, has emerged for the fabrication of electrospun PTFE fiber membranes [60]. This method utilizes the blending of water-soluble polymers (e.g., polyethylene oxide, polyvinyl alcohol) and water-insoluble PTFE for emulsion electrospinning to fabricate fibers [61]. Several studies have described the process of emulsion electrospinning [62–64]; a schematic illustration of the process is shown in Figure 4 [65]. During emulsion electrospinning, the resulting microstructure is the host water-soluble polymer fiber loaded with PTFE particles. A sintering step is usually done to remove the host water-soluble polymer and fuse the unspinnable PTFE particles into continuous fibers. Table 1 summarizes the emulsion electrospinning of PTFE fibers, their processing parameters, and fiber diameters.

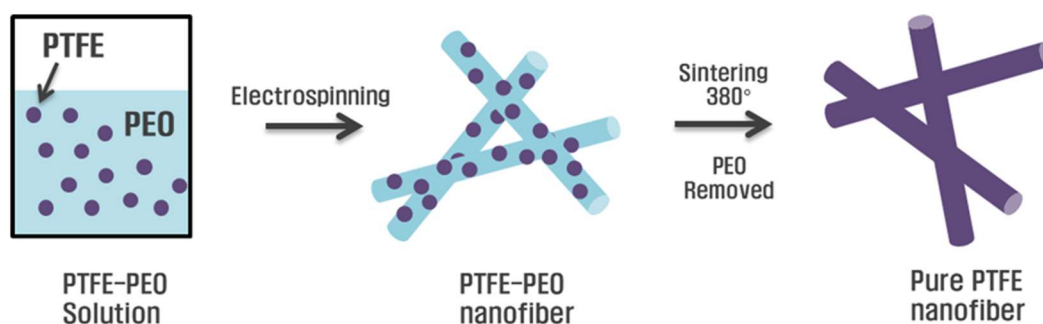


Figure 4. Schematic of emulsion electrospinning using polyethylene oxide (PEO) as the carrier for PTFE particles followed by a sintering process to remove the carrier and joining of the PTFE particles into solid fibers (Reproduced from Ref. [65] with permission).

Table 1. Emulsion electrospinning of PTFE fibers and fiber diameters.

PTFE/carrier ratio	Electrospinning parameters	Sintering temperature	Fiber diameter	Ref.
PTFE/PVA (70/30)	Voltage: 15 kV Spinning distance: 15 cm Flow rate: 0.01 mL/h	390 °C	300 nm without sintering	[63]
PTFE/PVA (14/1)	Voltage: 16 kV Spinning distance: 15 cm Flow rate: 0.4 mL/h	380 °C	506 nm, 8 h of sintering	[62]
PTFE/PEO (92/8)	Voltage: 10 kV Spinning distance: 12 cm Flow rate: 0.1 mL/h	340–400 °C	0.21 μm without sintering	[64]

Xiong et al. fabricated PTFE porous membranes by electrospinning [63]. PTFE was blended with PVA at different mass concentrations and blend ratios to study the effects of blend polymer ratios on fiber morphology and diameter. The fiber morphologies changed from bead-like to fibrous membranes when the amount of PVA in the blend fibers was increased. However, to have the maximum amount of PTFE in the fibers, the study suggested an optimum blend ratio of 30/70 for blend PVA/PTFE fibers. In addition, the effect of polymer concentration on the blend PVA/PTFE fibers showed bead-like fiber structures when polymer concentration was lower than 22%. As the polymer concentration increased, results showed continuous and uniform fibers with large diameters. There were no statistical differences in the average fiber diameters for those PVA/PTFE fibers obtained from solution concentrations of 22% or 26%. Using the optimum PVA/PTFE blend ratio of 30/70, a polymer solution was prepared for electrospinning at a concentration of 26% at voltage levels of 7, 9, 11, 13, and 15 kV with a tip-to-collector distance of 15 cm and a flow rate of 0.01 mL/min. When the electrospinning voltages were within the range of 7–11 kV, fiber diameter decreased from 550 to 420 nm. At higher electrospinning voltages, from 11 to 15 kV, there were minimal changes in the fiber diameter. Comparing the sintered fiber membranes to the pristine fiber membranes, the strength of the sintered fibers increased from 4 to 10 MPa, the elastic moduli of the sintered fibers increased from 22 to 260 MPa, and the failure strain of the sintered fibers increased from 63% to 69%. It was also determined that the appropriate sintering temperature range for the PVA/PTFE porous membranes was between 300 and 400 °C.

Qing et al. fabricated PTFE fibrous membranes by emulsion electrospinning using PVA as a carrier followed by a sintering process [62]. Standard single nozzle electrospinning was used to produce PVA/PTFE fibers with an applied voltage of 16 kV, a tip-to-collector distance of 15 cm, and a flow rate of 0.4 mL/h. The PTFE particles were evenly distributed in PVA host fibers followed by thermal sintering at 380 °C to obtain PTFE fibrous membranes. The sintered PTFE fibers had a tensile strength of 19.7 MPa, much higher than the tensile strength of the as-prepared PVA/PTFE fibers (7.5 MPa). The PTFE fibers had a fiber diameter of approximately 1 μm . The sintered PTFE fiber membrane was superhydrophobic with a water contact angle of 155°. The excellent corrosion resistance and the mechanical stability of PTFE fibers suggested the application in phase separation, where a gravity-driven oil/water separation test using the synthesized PTFE membranes showed a permeate flux of 1215 L/m²/h.

Zhao et al. fabricated PTFE fiber membranes using PEO as the polymer carrier followed by a sintering process to obtain PTFE fibrous membranes [59]. The electrospinning parameters of the PEO/PTFE fibers were 15 kV for the applied voltage, 15 cm for the tip-to-collector distance, and 0.5 mL/h for the flow rate. By transitioning the mixing weight ratio of PEO/PTFE from 0.07 to 0.12 in the blend PEO/PTFE fibers, the resulting fiber diameters increased from 700 to 1100 nm. This study demonstrated the use of PEO as a carrier to electrospun PTFE fibers with the correlations to polymer blending on the effects of average fiber diameter.

Su et al. fabricated hollow PTFE fiber membranes while investigating the fundamental electrospinning parameters including PTFE/PEO blending ratios and sintering temperatures [64]. The electrospinning process was performed at a flow rate of 0.1 mL/h, a tip-to-collector distance of 12 cm, and an applied voltage of 10 kV. Results from fiber surface morphology studies suggested that the optimized PTFE/PEO mass ratio was 92/8, much lower than the reported PTFE/PVA ratio of 70/30. Using PTFE/PEO at 92/8, the bead-to-string structures were eliminated where uniform and continuous fibers were observed. Sintering was done at four different temperatures (340, 360, 380, and 400 °C), with sintered membranes showing continuous fibers and typical fibrous web-like network structure. In addition, PTFE/PEO membrane sintered at 380 °C received the highest tensile strength, Young's modulus, and strain at break of 30.5 MPa, 53 MPa, and 315%, respectively.

Emulsion electrospinning followed by sintering can be used for near-field electrospinning (NFES). Cheng et al. developed a novel PTFE membrane with a regular geometric pore structure using the NFES method [66]. The process started with designing the membrane's pore geometry using computer-aided design software. The PTFE electrospinning solution included PTFE emulsion and an aqueous carrier of PVA solution to produce the electrospun PTFE/PVA membrane. The obtained PTFE/PVA membrane was sintered at a temperature of 380 °C. The electrospinning parameters used consisted of an applied voltage of 2.85 kV, a flow rate of 4.2 $\mu\text{L}/\text{min}$, and a spinneret-to-collector distance of 4 cm at $25 \pm 5^\circ\text{C}$ and relative humidity of $40\% \pm 10\%$. The study addressed the effects of sintering temperatures on the fiber morphology of the membranes.

TFE-based co-polymers can be electrospun into fibers due to their processing ability as melts/solutions, which is limited to perfluorinated solvents and electrospinning using the coaxial setup [67]. For example, Han and Steckl fabricated superhydrophobic and oleophobic core/shell fibers using polycaprolactone (PCL) as the core and Teflon AF 2400 as the shell [68]. The flow rates were 1.5 mL/h for the 10 wt% PCL in 2,2,2-trifluoroethanol core solution and 1.0 mL/h for the 1 wt% Teflon AF 2400 in FC-75 shell solution. The distance between the tip of the coaxial nozzle and the collector was 25 cm, and the applied voltage was 12.5 kV. The ambient temperature was between 70 and 75 °F, and relative humidity was between 20% and 45%. Results showed that PCL core solution

had a great effect on fiber diameter, where 10 wt% PCL core solution resulted in fiber diameters of 1–2 μm . At lower PCL core concentrations, beadings were found in the core/shell fiber mats. An increase in Teflon AF 2400 shell concentration also led to the formation of beads. The stiffness of the core/shell fiber membranes was 13 MPa, which was much lower than that of the Teflon AF 2400 films (i.e., 1.5 GPa). Also, core/shell fiber membranes had a lower ultimate tensile strength of 2.3 MPa as compared to that of the pristine PCL fiber membranes (i.e., 3.1 MPa).

5. Applications of electrospun PTFE fibers in membrane distillation

The use of electrospun fibers in MD has gained traction due to the development of emulsion electrospinning of hydrophobic PVDF materials, an important factor for achieving effective separation. Feng et al. electrospun PVDF fibrous membranes to produce drinking water from saline water through the air-gap membrane distillation technique [69]. The study reported a salt rejection rate of over 98% for a 6 wt% sodium chloride solution with fluxes ranging from 5 to 28 $\text{kg}/\text{m}^2/\text{h}$, where higher temperature differences resulted in higher fluxes. To reduce the energy consumption in MD, Prince et al. incorporated clay nanocomposites into the electrospun PVDF fibers [70]. The clay-PVDF composite membranes substantially increased the water contact angle to 154.2° . However, the clay-PVDF composite membranes had a relatively low water flux of less than $5.5 \text{ kg}/\text{m}^2/\text{h}$. This study demonstrated a well-known trade-off effect in membrane fabrication and distillation, namely the inverse relationship between hydrophobicity and permeation rates of the membranes.

Although electrospun PVDF fibrous membranes were first reported to be used in a membrane distillation process, other hydrophobic polymers, such as PP, polyethylene (PE), and PTFE, were reviewed for potential applications in membrane distillation [71]. Among these polymers, PTFE stands out as the most ideal polymer for electrospun fibers in membrane distillation since PTFE has the highest hydrophobicity and the least surface energy at 9–20 mN/m due to its carbon backbone and fluorinated side groups. Table 2 summarizes the electrospun PTFE fibers and their performances in membrane distillation.

To solve the problem of low water flux in various electrospun fibrous membranes, Dong et al. fabricated a superhydrophobic PVDF-PTFE electrospun fibrous membranes with a high water flux by incorporating PTFE into the PVDF dope solution to improve the surface hydrophobicity of the membrane [10]. The inclusion of PTFE into the PVDF matrix not only increased the hydrophobicity (e.g., water contact angles up to 152.2°) but also significantly improved water flux ($18.5 \text{ kg}/\text{m}^2/\text{h}$) and salt rejection (99.9%) when tested with a 3.5 wt% sodium chloride feed solution. To produce the PVDF-PTFE electrospun fibrous membranes, an applied voltage of 18 kV, a flow rate of 0.5 mL/h , and a tip-to-collector distance of 15 cm were used under a relative humidity of $50\% \pm 5\%$ and an ambient temperature of $25 \pm 1^\circ\text{C}$. Results showed that increasing PTFE contents in the PVDF-PTFE fibers from 0% to 12% increased the water contact angles from 130.4 to 152.2° and the liquid entry pressure from 84 to 137 kPa. Using a feed solution of 3.5 wt% NaCl, the reported permeation flux was $18.5 \text{ kg}/\text{m}^2/\text{h}$, which was higher than those of commercial PTFE membrane membranes under similar circumstances ($\sim 15 \text{ kg}/\text{m}^2/\text{h}$). In addition, the salt rejection rate was around 99.9% in 15 h, suggesting the viability of the fibrous membranes for commercial applications. This finding highlights the importance of composite membrane systems in overcoming the flux limitations typically observed in pure polymer membranes. Their study brought attention to the optimization of the PTFE concentration

in the PVDF-PTFE blend fibers, as higher PTFE concentrations in the blend fibers resulted in a higher liquid entry pressure and more hydrophobic surfaces (e.g., increased water angles).

PTFE has the highest hydrophobicity among all hydrophobic polymers. In addition, PTFE's properties, namely being environmentally benign, inert, and mechanically stable and having high resistance to UV and oxidation by radicals and malleability, make it an ideal candidate for membrane distillation applications [72,73]. PTFE fibrous membranes are suitable supports for titanium oxide particles, which indicates potential optoelectronic applications in membrane distillation applications. Reports showed that titanium oxide had a large excitation binding energy of 60 meV with a wide band gap of 3.3 eV at 300 K [74,75].

Huang et al. electrospun PTFE/PVA/zinc acetate composite membranes to evaluate the photocatalytic rejection of wastewater discharge while investigating the self-cleaning performance of the composite membrane by reporting rejection and permeate flux recovery in vacuum distillation [76]. Electrospinning of the fiber composites was performed at 25 kV, a tip-to-collector distance of 10 cm, and a flow rate of 0.008 mL/min. The resulting electrospun fiber composites were sintered at 380 °C to remove the PVA carrier and to introduce the ZnO particles. The reported self-cleaning performances of PTFE/ZnO membranes using rejection and permeate flux recovery in vacuum membrane distillation assays under UV irradiation showed a salt rejection of 99.7% using a flux of 16.5 L/m²/h. Despite the reduction in flux and salt rejection in time, the fouled membrane could be cleaned after 3 h with a permeate flux recovery rate of more than 94%. The dye removal rate was up to 45% after 10 h of operation. The ability of self-cleaning provides an alternative to solve the problem of fouling and scaling, which are common challenges in MD systems. The use of ZnO nanoparticles provides a dual benefit to MD, including the improvement of both the hydrophobicity of the membrane and its ability to degrade contaminants on the membrane surface to enhance the membrane's longevity to reduce maintenance requirements.

Despite the advantages of strong hydrophobic nature, PTFE membranes are susceptible to scaling or wetting by organic contaminants or hypersaline solutions leading to a decrease in salt rejection [77]. This effect is due to the presence of amphiphilic organic compounds in the feed solution. To solve this problem, Xu et al. co-electrospun PTFE/PVA and polyacrylonitrile (PAN) to produce amphiphilic PTFE fibrous membranes with great anti-fouling and anti-wetting properties [78]. The electrospinning conditions included an applied voltage of 25 ± 0.2 kV, a spinning distance of 10.0 ± 0.5 cm, and a flow rate of 0.48 mL/h for PTFE/PVA solution and 0.48 mL/h for PAN solution. After electrospinning, the fibers were sintered at 380 °C to remove PVA. To make the fibrous membrane amphiphilic, silicon dioxide nanoparticles were fixed on PAN and PTFE fibers followed by fluorination with trimethoxy (1H,1H,2H,2H-heptadecafluorodecyl) silane (17-FAS). These nanoparticles had a high surface roughness and low surface energy to repel liquids with low surface tension [77]. To investigate the amphiphilic nature of the PTFE/SiO₂ fibrous membranes, the water contact angle was 166.9°, and the oil contact angle was 134.5°. The PTFE/SiO₂ fibrous membranes maintained a stable membrane distillation flux of 17.09 L/m²/h and a salt rejection rate higher than 99.96% during the 24 h operation. The reported permeate flux was 6.91 L/m²/h in the presence of sodium dodecyl sulfate, suggesting anti-wetting properties. This work highlights the importance of electrospinning amphiphilic membranes that were able to resist fouling, thereby improving the operational lifetime of MD systems in diverse feedwater conditions.

To overcome the fouling and wetting properties of the fibrous membranes, Ju et al. electrospun hydrophobic 8 vinyl-grafted polyhedral oligomeric silsesquioxane (vinyl-POSS) nanoparticles with

PTFE fibers [79]. POSS nanoparticles have hollow rigid cage or semi-cage structures consisting of organic-inorganic hybrid segments [80]. The eight vertices attached to the organic segments ($-\text{CH}=\text{CH}_2$) in the POSS nanoparticles make them highly compatible with polymer matrix as compared to the traditional inorganic silicon dioxide nanoparticles [81]. As such, POSS/polymer fibrous membranes have attracted much attention in membrane distillation applications. In the reported study, POSS/PTFE/PVA fibers were electrospun using an applied voltage of 28 kV, a flow rate of 1.0 mL/h, and a tip-to-collector distance of 18 cm under a temperature of 25 ± 5 °C and a relative humidity of $35\% \pm 5\%$ followed by a sintering temperature of 390 °C to remove PVA. The resulting POSS/PTFE fibrous membranes had a water contact angle of $151 \pm 4^\circ$. The water flux was 40 ± 2 L/m²/h when the feed and permeate temperatures were 60 and 20 °C, exhibiting excellent long-term stability in the 200-hour direct-contact membrane distillation process. This ability suggests that POSS could play a crucial role in enhancing both the flux and durability of MD membranes.

Recently, a novel approach to the development of fibrous membranes in MD was reported by electrospinning of PTFE fibers without the inclusion of nanoparticles in the fibrous membranes. Liu et al. used a low-temperature crosslinking and fluorination approach to produce PTFE/PVA fibers for surface property modifications [82]. Their PTFE fibrous membranes demonstrated robust amphiphobicity with a water contact angle of 155.2° and an oil contact angle of 132.7° . PTFE fibrous membranes showed stable permeation flux of 52.1 and 26.7 L/m²/h when feeding with 3.5 and 25.0 wt% sodium chloride solutions, respectively. The reported salt rejection performance was at and/or above 99.99% at a continuous operation for 24 h, demonstrating exceptional anti-scaling performance. This article indicated further applications of MD in salt feeds containing sodium dodecyl sulfate (SDS) or diesel oil with robust anti-wetting and anti-fouling properties. It demonstrated the effectiveness of seawater desalination across diverse concentrations of inorganic salts. This work demonstrated a system for the development of cost-effective, hyper-salinity-resistant, and reliable MD desalination systems.

Table 2. Electrospun PTFE fibrous membranes in MD.

Polymer/Carrier	Parameter	MD performance	Ref.
PTFE/PVDF	Voltage: 18 kV	Permeate flux: 18.5 kg/m ²	[10]
	Spinning distance: 15 cm	Salt rejection: 99.9%	
	Flow rate: 0.5 mL/h		
PTFE/PVA/zinc acetate	Voltage: 18 kV	Permeate flux: 16.5 L/m ² /h	[76]
	Spinning distance: 10 cm	Salt rejection: 99.7%	
	Flow rate: 0.008 mL/min		
PTFE/PVA/PAN	Voltage: 25 kV	Permeate flux: 17.09 L/m ² /h	[78]
	Spinning distance: 10 cm	Salt rejection: 99.6%	
	Flow rate: 0.48 mL/h		

6. Conclusions and future directions

In general, electrospun PTFE fibrous membranes represent a great advancement in membrane distillation with their excellent hydrophobicity and chemical inertness. One of the notable strengths of electrospun PTFE membranes lies in their high pore interconnectivity and relatively uniform pore size distribution, both of which are pivotal for improved membrane performance in distillation. This review

addresses the molecular structure of PTFE, electrospinning of PTFE fibers, and their applications in membrane distillation. The high surface area of PTFE fibers makes them easily functional, allowing for customization to fit specific conditions in membrane distillation. These functional modifications include nanoparticle coating, chemical treatment, heat treatment, grafting, and interfacial polymerization to improve membrane distillation efficiency and reduce wetting and fouling of the membranes. Despite these advantages of electrospun PTFE fibers in membrane distillation, there are still scientific bottlenecks to improving fiber morphologies and membrane structures to avoid microcracking and temperature-induced defects. In addition, large-scale commercialization and manufacturing quality controls remain a technical challenge in the scientific field. Overall, our review provides a scientific understanding of the electrospinning of PTFE fibers and the engineering application of these fibers in membrane distillation.

Use of AI tools declaration

The authors declare they have not used Artificial Intelligence (AI) tools in the creation of this article.

Acknowledgments

We would like to thank Dr. Zishu Cao from the Department of Chemical Engineering, College of Engineering, at The University of Texas at Tyler for supervising and mentoring of Mr. Charles Defor. The authors thank the Department of Mechanical Engineering, College of Engineering, at The University of Texas at Tyler for supporting the work.

Author contributions

Conceptualization: C.D. and S-F.C.; literature review: C.D.; writing—original draft preparation: C.D.; writing—review & editing: S-F.C.; supervision: S-F.C.; project administration: S-F.C.

Conflict of interest

The authors declare no conflict of interest.

References

1. Shyr TW, Chung WC, Lu WL, et al. (2015) Unusually high temperature transition and microporous structure of polytetrafluoroethylene fibre prepared through film fibrillation. *Eur Polym J* 72: 50–63. <https://doi.org/10.1016/j.eurpolymj.2015.08.017>
2. Xu A, Li H, Yuan WZ, et al. (2012) Radical homopolymerization of tetrafluoroethylene initiated by perfluorodiacyl peroxide in supercritical carbon dioxide: Reaction mechanism and initiation kinetics. *Eur Polym J* 48: 1431–1438. <https://doi.org/10.1016/j.eurpolymj.2012.05.012>
3. Clark ES (1999) The molecular conformations of polytetrafluoroethylene: Forms II and IV. *Polymer* 40: 4659–4665. [https://doi.org/10.1016/S0032-3861\(99\)00109-3](https://doi.org/10.1016/S0032-3861(99)00109-3)

4. Puts GJ, Crouse P, Ameduri BM (2019) Polytetrafluoroethylene: Synthesis and characterization of the original extreme polymer. *Chem Rev* 119: 1763–1805. <https://doi.org/10.1021/acs.chemrev.8b00458>
5. Biswas SK, Vijayan K (1992) Friction and wear of PTFE—A review. *Wear* 158: 193–211. [https://doi.org/10.1016/0043-1648\(92\)90039-B](https://doi.org/10.1016/0043-1648(92)90039-B)
6. Dhanumalayan E, Joshi GM (2018) Performance properties and applications of polytetrafluoroethylene (PTFE)—A review. *Adv Compos Hybrid Mater* 1: 247–268. <https://doi.org/10.1007/s42114-018-0023-8>
7. Lu X, Peng Y, Ge L, et al. (2016) Amphiphobic PVDF composite membranes for anti-fouling direct contact membrane distillation. *J Membr Sci* 505: 61–69. <https://doi.org/10.1016/j.memsci.2015.12.042>
8. Alessandro F, Macedonio F, Drioli E (2023) New materials and phenomena in membrane distillation. *Chemistry* 5: 65–84. <https://doi.org/10.3390/chemistry5010006>
9. Li X, Yu X, Cheng C, et al. (2015) Electrospun superhydrophobic organic/inorganic composite nanofibrous membranes for membrane distillation. *ACS Appl Mater Interfaces* 7: 21919–21930. <https://doi.org/10.1021/acsami.5b06509>
10. Dong ZQ, Ma X, Xu ZL, et al. (2014) Superhydrophobic PVDF–PTFE electrospun nanofibrous membranes for desalination by vacuum membrane distillation. *Desalination* 347: 175–183. <https://doi.org/10.1016/j.desal.2014.05.015>
11. Nthunya LN, Gutierrez L, Derese S, et al. (2019) A review of nanoparticle-enhanced membrane distillation membranes: Membrane synthesis and applications in water treatment. *J Chem Technol Biotechnol* 94: 2757–2771. <https://doi.org/10.1002/jctb.5977>
12. Efome JE, Rana D, Matsuura T, et al. (2016) Enhanced performance of PVDF nanocomposite membrane by nanofiber coating: A membrane for sustainable desalination through MD. *Water Res* 89: 39–49. <https://doi.org/10.1016/j.watres.2015.11.040>
13. Feng S, Zhong Z, Wang Y, et al. (2018) Progress and perspectives in PTFE membrane: Preparation, modification, and applications. *J Membr Sci* 549: 332–349. <https://doi.org/10.1016/j.memsci.2017.12.032>
14. Huang QL, Xiao C, Feng X, et al. (2013) Design of super-hydrophobic microporous polytetrafluoroethylene membranes. *New J Chem* 37: 373–379. <https://doi.org/10.1039/C2NJ40355B>
15. Li L, Sirkar KK (2016) Influence of microporous membrane properties on the desalination performance in direct contact membrane distillation. *J Membr Sci* 513: 280–293. <https://doi.org/10.1021/acsami.5b06509>
16. Yang Y, Strobel M, Kirk S, et al. (2010) Fluorine plasma treatments of poly(propylene) films, 2—Modeling reaction mechanisms and scaling. *Plasma Process Polym* 7: 123–150. <https://doi.org/10.1002/ppap.200900114>
17. Bottino A, Capannelli G, Comite A, et al. (2015) Novel polytetrafluoroethylene tubular membranes for membrane distillation. *Desalination Water Treat* 53: 1559–1564. <https://doi.org/10.1080/19443994.2014.982955>
18. Reza Shirzad Kebria M, Rahimpour A (2020) Membrane distillation: Basics, advances, and applications, In: Abdelrasoul A, *Advances in Membrane Technologies*, Rijeka: IntechOpen, 67–87. <https://doi.org/10.5772/intechopen.86952>

19. Xu H, Jin W, Wang F, et al. (2018) Preparation and properties of PTFE hollow fiber membranes for the removal of ultrafine particles in PM_{2.5} with repetitive usage capability. *RSC Adv* 8: 38245–38258. <https://doi.org/10.1039/C8RA07789D>
20. Lu W, Yuan Z, Zhao Y, et al. (2017) Porous membranes in secondary battery technologies. *Chem Soc Rev* 46: 2199–2236. <https://doi.org/10.1039/C6CS00823B>
21. Gu M, Zhang J, Wang X, et al. (2006) Formation of poly(vinylidene fluoride) (PVDF) membranes via thermally induced phase separation. *Desalination* 192: 160–167. <https://doi.org/10.1016/j.desal.2005.10.015>
22. Karimi H, Rahimpour A, Shirzad Kebria MR (2016) Pesticides removal from water using modified piperazine-based nanofiltration (NF) membranes. *Desalination Water Treat* 57: 24844–24854. <https://doi.org/10.1080/19443994.2016.1156580>
23. Mahdi A Shirazi M, Bazgir S, Meshkani F (2020) Electrospun nanofibrous membranes for water treatment, In: Abdelrasoul A, *Advances in Membrane Technologies*, Rijeka: IntechOpen. <https://doi.org/10.5772/intechopen.87948>
24. Shirazi MMA, Asghari M (2018) Electrospun filters for oil–water separation, In: Focarete ML, Gualandi C, Ramakrishna S, *Filtering Media by Electrospinning*, Cham: Springer International Publishing, 151–173. https://doi.org/10.1007/978-3-319-78163-1_7
25. Emerine R, Chou SF (2022) Fast delivery of melatonin from electrospun blend polyvinyl alcohol and polyethylene oxide (PVA/PEO) fibers. *AIMS Bioeng* 9: 178–196. <https://doi.org/10.3934/bioeng.2022013>
26. Hawkins BC, Burnett E, Chou SF (2022) Physicomechanical properties and in vitro release behaviors of electrospun ibuprofen-loaded blend PEO/EC fibers. *Mater Today Commun* 30: 103205. <https://doi.org/10.1016/j.mtcomm.2022.103205>
27. Faglie A, Emerine R, Chou SF (2023) Effects of poloxamers as excipients on the physicomechanical properties, cellular biocompatibility, and in vitro drug release of electrospun polycaprolactone (PCL) fibers. *Polymers* 15: 2997. <https://doi.org/10.3390/polym15142997>
28. Gizaw M, Bani Mustafa D, Chou SF (2023) Fabrication of drug-eluting polycaprolactone and chitosan blend microfibers for topical drug delivery applications. *Front Mater* 10: 1144752. <https://doi.org/10.3389/fmats.2023.1144752>
29. Bani Mustafa D, Sakai T, Sato O, et al. (2024) Electrospun ibuprofen-loaded blend PCL/PEO fibers for topical drug delivery applications. *Polymers* 16: 1934. <https://doi.org/10.3390/polym16131934>
30. Mohamed R, Chou SF (2024) Physicomechanical characterizations and in vitro release studies of electrospun ethyl cellulose fibers, solvent cast carboxymethyl cellulose films, and their composites. *Int J Biol Macromol* 267: 131374. <https://doi.org/10.1016/j.ijbiomac.2024.131374>
31. Subbiah T, Bhat GS, Tock RW, et al. (2005) Electrospinning of nanofibers. *J Appl Polym Sci* 96: 557–569. <https://doi.org/10.1002/app.21481>
32. Formhals A (1934) Process and apparatus for preparing artificial threads.
33. Taylor GI (1969) Electrically driven jets. *Proc R Soc Lond Math Phys Sci* 313: 453–475. <https://doi.org/10.1098/rspa.1969.0205>
34. Huang ZM, Zhang YZ, Kotaki M, et al. (2003) A review on polymer nanofibers by electrospinning and their applications in nanocomposites. *Compos Sci Technol* 63: 2223–2253. [https://doi.org/10.1016/S0266-3538\(03\)00178-7](https://doi.org/10.1016/S0266-3538(03)00178-7)

35. Wang X, Hsiao BS (2016) Electrospun nanofiber membranes. *Curr Opin Chem Eng* 12: 62–81. <https://doi.org/10.1016/j.coche.2016.03.001>
36. Beachley V, Wen X (2009) Effect of electrospinning parameters on the nanofiber diameter and length. *Mater Sci Eng C* 29: 663–668. <https://doi.org/10.1016/j.msec.2008.10.037>
37. Yördem OS, Papila M, Menceloğlu YZ (2008) Effects of electrospinning parameters on polyacrylonitrile nanofiber diameter: An investigation by response surface methodology. *Mater Des* 29: 34–44. <https://doi.org/10.1016/j.matdes.2006.12.013>
38. Zhang C, Yuan X, Wu L, et al. (2005) Study on morphology of electrospun poly(vinyl alcohol) mats. *Eur Polym J* 41: 423–432. <https://doi.org/10.1016/j.eurpolymj.2004.10.027>
39. Zargham S, Bazgir S, Tavakoli A, et al. (2012) The effect of flow rate on morphology and deposition area of electrospun nylon 6 nanofiber. *J Eng Fibers Fabr* 7: 42–49. <https://doi.org/10.1177/155892501200700414>
40. Homayoni H, Ravandi SAH, Valizadeh M (2009) Electrospinning of chitosan nanofibers: Processing optimization. *Carbohydr Polym* 77: 656–661. <https://doi.org/10.1016/j.carbpol.2009.02.008>
41. Tan SH, Inai R, Kotaki M, et al. (2005) Systematic parameter study for ultra-fine fiber fabrication via electrospinning process. *Polymer* 46: 6128–6134. <https://doi.org/10.1016/j.polymer.2005.05.068>
42. Liu Y, He J, Yu J, et al. (2008) Controlling numbers and sizes of beads in electrospun nanofibers. *Polym Int* 57: 632–636. <https://doi.org/10.1002/pi.2387>
43. He JH, Wan YQ, Yu JY (2008) Effect of concentration on electrospun polyacrylonitrile (PAN) nanofibers. *Fibers Polym* 9: 140–142. <https://doi.org/10.1007/s12221-008-0023-3>
44. Koski A, Yim K, Shivkumar S (2004) Effect of molecular weight on fibrous PVA produced by electrospinning. *Mater Lett* 58: 493–497. [https://doi.org/10.1016/S0167-577X\(03\)00532-9](https://doi.org/10.1016/S0167-577X(03)00532-9)
45. Mit-uppatham C, Nithitanakul M, Supaphol P (2004) Ultrafine electrospun polyamide-6 fibers: Effect of solution conditions on morphology and average fiber diameter. *Macromol Chem Phys* 205: 2327–2338. <https://doi.org/10.1002/macp.200400225>
46. Jarusuwannapoom T, Hongrojjanawiwat W, Jitjaicham S, et al. (2005) Effect of solvents on electro-spinnability of polystyrene solutions and morphological appearance of resulting electrospun polystyrene fibers. *Eur Polym J* 41: 409–421. <https://doi.org/10.1016/j.eurpolymj.2004.10.010>
47. Jia L, Qin X (2013) The effect of different surfactants on the electrospinning poly(vinyl alcohol) (PVA) nanofibers. *J Therm Anal Calorim* 112: 595–605. <https://doi.org/10.1007/s10973-012-2607-9>
48. Fan L, Xu Y, Zhou X, et al. (2018) Effect of salt concentration in spinning solution on fiber diameter and mechanical property of electrospun styrene-butadiene-styrene tri-block copolymer membrane. *Polymer* 153: 61–69. <https://doi.org/10.1016/j.polymer.2018.08.008>
49. Qin X, Yang E, Li N, et al. (2007) Effect of different salts on electrospinning of polyacrylonitrile (PAN) polymer solution. *J Appl Polym Sci* 103: 3865–3870. <https://doi.org/10.1002/app.25498>
50. Uyar T, Besenbacher F (2008) Electrospinning of uniform polystyrene fibers: The effect of solvent conductivity. *Polymer* 49: 5336–5343. <https://doi.org/10.1016/j.polymer.2008.09.025>
51. Tungprapa S, Puangparn T, Weerasombut M, et al. (2007) Electrospun cellulose acetate fibers: Effect of solvent system on morphology and fiber diameter. *Cellulose* 14: 563–575. <https://doi.org/10.1007/s10570-007-9113-4>

52. Huan S, Liu G, Han G, et al. (2015) Effect of experimental parameters on morphological, mechanical and hydrophobic properties of electrospun polystyrene fibers. *Materials* 8: 2718–2734. <https://doi.org/10.3390/ma8052718>
53. Moomand K, Lim LT (2015) Effects of solvent and n-3 rich fish oil on physicochemical properties of electrospun zein fibres. *Food Hydrocoll* 46: 191–200. <https://doi.org/10.1016/j.foodhyd.2014.12.014>
54. Song Z, Chiang SW, Chu X, et al. (2018) Effects of solvent on structures and properties of electrospun poly(ethylene oxide) nanofibers. *J Appl Polym Sci* 135: 45787. <https://doi.org/10.1002/app.45787>
55. De Vrieze S, Van Camp T, Nelvig A, et al. (2009) The effect of temperature and humidity on electrospinning. *J Mater Sci* 44: 1357–1362. <https://doi.org/10.1007/s10853-008-3010-6>
56. Hardick O, Stevens B, Bracewell DG (2011) Nanofibre fabrication in a temperature and humidity controlled environment for improved fibre consistency. *J Mater Sci* 46: 3890–3898. <https://doi.org/10.1007/s10853-011-5310-5>
57. Hunke H, Soin N, Shah T, et al. (2015) Influence of plasma pre-treatment of polytetrafluoroethylene (PTFE) micropowders on the mechanical and tribological performance of polyethersulfone (PESU)–PTFE composites. *Wear* 328–329: 480–487. <https://doi.org/10.1016/j.wear.2015.03.004>
58. Hunke H, Soin N, Shah T, et al. (2015) Low-pressure H₂, NH₃ microwave plasma treatment of polytetrafluoroethylene (PTFE) powders: Chemical, thermal and wettability analysis. *Materials* 8: 2258–2275. <https://doi.org/10.3390/ma8052258>
59. Zhao P, Soin N, Prashanthi K, et al. (2018) Emulsion electrospinning of polytetrafluoroethylene (PTFE) nanofibrous membranes for high-performance triboelectric nanogenerators. *ACS Appl Mater Interfaces* 10: 5880–5891. <https://doi.org/10.1021/acsami.7b18442>
60. Yazgan G, Popa AM, Rossi RM, et al. (2015) Tunable release of hydrophilic compounds from hydrophobic nanostructured fibers prepared by emulsion electrospinning. *Polymer* 66: 268–276. <https://doi.org/10.1016/j.polymer.2015.04.045>
61. Akduman C (2023) Preparation and comparison of electrospun PEO/PTFE and PVA/PTFE nanofiber membranes for syringe filters. *J Appl Polym Sci* 140: e54344. <https://doi.org/10.1002/app.54344>
62. Qing W, Shi X, Deng Y, et al. (2017) Robust superhydrophobic-superoleophilic polytetrafluoroethylene nanofibrous membrane for oil/water separation. *J Membr Sci* 540: 354–361. <https://doi.org/10.1016/j.memsci.2017.06.060>
63. Xiong J, Huo P, Ko FK (2009) Fabrication of ultrafine fibrous polytetrafluoroethylene porous membranes by electrospinning. *J Mater Res* 24: 2755–2761. <https://doi.org/10.1557/jmr.2009.0347>
64. Su C, Li Y, Cao H, et al. (2019) Novel PTFE hollow fiber membrane fabricated by emulsion electrospinning and sintering for membrane distillation. *J Membr Sci* 583: 200–208. <https://doi.org/10.1016/j.memsci.2019.04.037>
65. Son SJ, Hong SK, Lim G (2020) Emulsion electrospinning of hydrophobic PTFE-PEO composite nanofibrous membranes for simple oil/water separation. *J Sens Sci Technol* 29: 89–92. <https://doi.org/10.5369/JSST.2020.29.2.89>

66. Cheng J, Huang Q, Huang Y, et al. (2020) Study on a novel PTFE membrane with regular geometric pore structures fabricated by near-field electrospinning, and its applications. *J Membr Sci* 603: 118014. <https://doi.org/10.1016/j.memsci.2020.118014>
67. Kianfar P, Bongiovanni R, Ameduri B, et al. (2023) Electrospinning of fluorinated polymers: Current state of the art on processes and applications. *Polym Rev* 63: 127–199. <https://doi.org/10.1080/15583724.2022.2067868>
68. Han D, Steckl AJ (2009) Superhydrophobic and oleophobic fibers by coaxial electrospinning. *Langmuir* 25: 9454–9462. <https://doi.org/10.1021/la900660v>
69. Feng C, Khulbe KC, Matsuura T, et al. (2008) Production of drinking water from saline water by air-gap membrane distillation using polyvinylidene fluoride nanofiber membrane. *J Membr Sci* 311: 1–6. <https://doi.org/10.1016/j.memsci.2007.12.026>
70. Prince JA, Singh G, Rana D, et al. (2012) Preparation and characterization of highly hydrophobic poly(vinylidene fluoride)—Clay nanocomposite nanofiber membranes (PVDF–clay NNMs) for desalination using direct contact membrane distillation. *J Membr Sci* 397–398: 80–86. <https://doi.org/10.1016/j.memsci.2012.01.012>
71. Wang P, Chung TS (2015) Recent advances in membrane distillation processes: Membrane development, configuration design and application exploring. *J Membr Sci* 474: 39–56. <https://doi.org/10.1016/j.memsci.2014.09.016>
72. Singh S, Mahalingam H, Singh PK (2013) Polymer-supported titanium dioxide photocatalysts for environmental remediation: A review. *Appl Catal Gen* 462–463: 178–195. <https://doi.org/10.1016/j.apcata.2013.04.039>
73. Pei CC, Leung WWF (2013) Enhanced photocatalytic activity of electrospun TiO₂/ZnO nanofibers with optimal anatase/rutile ratio. *Catal Commun* 37: 100–104. <https://doi.org/10.1016/j.catcom.2013.03.029>
74. Sankapal BR, Lux-Steiner MCh, Ennaoui A (2005) Synthesis and characterization of anatase-TiO₂ thin films. *Appl Surf Sci* 239: 165–170. <https://doi.org/10.1016/j.apsusc.2004.05.142>
75. Bozzi A, Yuranova T, Kiwi J (2005) Self-cleaning of wool-polyamide and polyester textiles by TiO₂-rutile modification under daylight irradiation at ambient temperature. *J Photochem Photobiol Chem* 172: 27–34. <https://doi.org/10.1016/j.jphotochem.2004.11.010>
76. Huang QL, Huang Y, Xiao CF, et al. (2017) Electrospun ultrafine fibrous PTFE-supported ZnO porous membrane with self-cleaning function for vacuum membrane distillation. *J Membr Sci* 534: 73–82. <https://doi.org/10.1016/j.memsci.2017.04.015>
77. Saffarini RB, Mansoor B, Thomas R, et al. (2013) Effect of temperature-dependent microstructure evolution on pore wetting in PTFE membranes under membrane distillation conditions. *J Membr Sci* 429: 282–294. <https://doi.org/10.1016/j.memsci.2012.11.049>
78. Xu M, Cheng J, Du X, et al. (2022) Amphiphobic electrospun PTFE nanofibrous membranes for robust membrane distillation process. *J Membr Sci* 641: 119876. <https://doi.org/10.1016/j.memsci.2021.119876>
79. Ju J, Fejjari K, Cheng Y, et al. (2020) Engineering hierarchically structured superhydrophobic PTFE/POSS nanofibrous membranes for membrane distillation. *Desalination* 486: 114481. <https://doi.org/10.1016/j.desal.2020.114481>
80. Lu C, Su C, Cao H, et al. (2018) F-POSS based omniphobic membrane for robust membrane distillation. *Mater Lett* 228: 85–88. <https://doi.org/10.1016/j.matlet.2018.05.126>

81. Bharadwaj RK, Berry RJ, Farmer BL (2000) Molecular dynamics simulation study of norbornene–POSS polymers. *Polymer* 41: 7209–7221. [https://doi.org/10.1016/S0032-3861\(00\)00072-0](https://doi.org/10.1016/S0032-3861(00)00072-0)
82. Liu Y, Meng Z, Zou R, et al. (2024) Crosslinking and fluorination reinforced PTFE nanofibrous membrane with excellent amphiphobic performance for low-scaling membrane distillations. *Water Res* 256: 121594. <https://doi.org/10.1016/j.watres.2024.121594>



AIMS Press

© 2024 the Author(s), licensee AIMS Press. This is an open access article distributed under the terms of the Creative Commons Attribution License (<https://creativecommons.org/licenses/by/4.0>)